# COMPARISON OF CASCADED H-BRIDGE CONVERTERS AND MODULAR MULTILEVEL CONVERTERS FOR THE USE IN MEDIUM VOLTAGE GRID CONNECTED BATTERY ENERGY STORAGE SYSTEMS

Lennart BARUSCHKA
Leibniz University of Hannover – Germany
baruschka@ial.uni-hannover.de

Axel MERTENS
Leibniz University of Hannover – Germany
mertens@ial.uni-hannover.de

## *ABSTRACT*

*In this paper, the Cascaded H-Bridge (CHB) converter is compared to the Modular Multilevel Converter (M²LC) regarding their efficiency and use of active and passive components. Design guidelines are developed.*

## INTRODUCTION

In recent years, the amount of energy decentrally "harvested" from renewable sources has been growing continously. In order to overcome problems in the transportation grid, Battery Energy Storage Systems (BESS) will play an increasing role in future energy systems.
Today, most storage systems use two- or three-level inverters. However, these are surpassed by modular multilevel topologies that provide benefits in terms of higher effective output frequency at a lower switching frequency, scalable design and error handling capability. The CHB (fig. 1) has already been proposed to be used as an inverter for BESS[5]. In this paper, it is compared to the M²LC, a topology mostly used for HVDC purposes[4]. Variants enabling step-up operation are included into the examination.
The inverter ratings used for the numerical evaluation are given in table 1. The inverter should be directly connected to the grid without an expensive and bulky transformer.
The maximum peak output voltage and current are

$$\hat{v}_{\mathrm{o,max}} = \sqrt{\frac{2}{3}} a_{\mathrm{ov}} a_{\mathrm{vctrl}} v_{\mathrm{LL,N}} = 19.76\ \mathrm{kV} \quad (1)$$

$$\hat{i}_{\mathrm{o,max}} = \sqrt{\frac{2}{3}} \frac{P_{\mathrm{inv}}}{a_{\mathrm{uv}} v_{\mathrm{LL,N}}} = 480\ \mathrm{A} \quad . \quad (2)$$

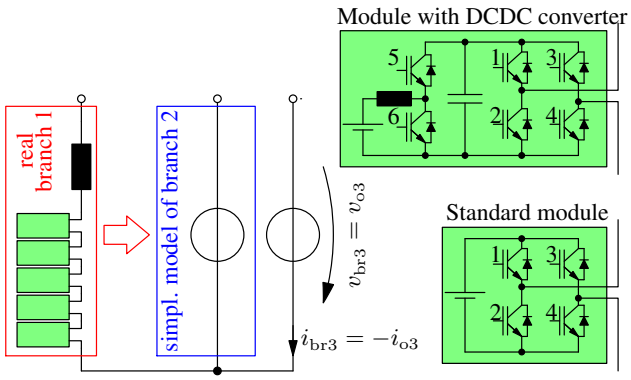


Figure 1: CHB topology, its analytic simplified model and its battery modules

| Description | Symbol | Value |
|---|---|---|
| apparent power | $S_{\mathrm{inv}}$ | 10 MVA |
| grid line-to-line voltage | $v_{\mathrm{LL,N}}$ | 20 kV |
| switching frequency | $f_{\mathrm{s}}$ | 750 Hz |
| grid undervoltage[1] | $a_{\mathrm{uv}}$ | 0.85 |
| grid overvoltage[1] | $a_{\mathrm{ov}}$ | 1.1 |
| voltage reserve for controller | $a_{\mathrm{vctrl}}$ | 1.1 |
| DCDC voltage reserve | $a_{\mathrm{bsm}}$ | 0.98 |
| voltage variation in modules | $a_{\Delta\mathrm{vcap}}$ | 1.2 |
| min. battery cell voltage[7] | $v_{\mathrm{cell,min}}$ | 1.75 V |
| nominal battery cell voltage[7] | $v_{\mathrm{cell,N}}$ | 2 V |
| max. battery cell voltage[7] | $v_{\mathrm{cell,max}}$ | 2.45 V |

Table 1: Parameters used for dimensioning example

## SIMPLIFIED MODELS

Both modular multilevel inverters consist of 3 or 6 branches that incorporate several identical cells functioning as switchable voltage sources. The cells with full-bridge outputs can supply $+v_{\mathrm{cap}}$, 0 and $-v_{\mathrm{cap}}$ at their terminals, the cells with half-bridge outputs $+v_{\mathrm{cap}}$ and 0.
The control pattern used to balance the energy among the modules and adjust the branch set-point voltage has been discussed before[3, 6, 8] and will not be regarded here. For the calculations, it is assumed that all modules operate at

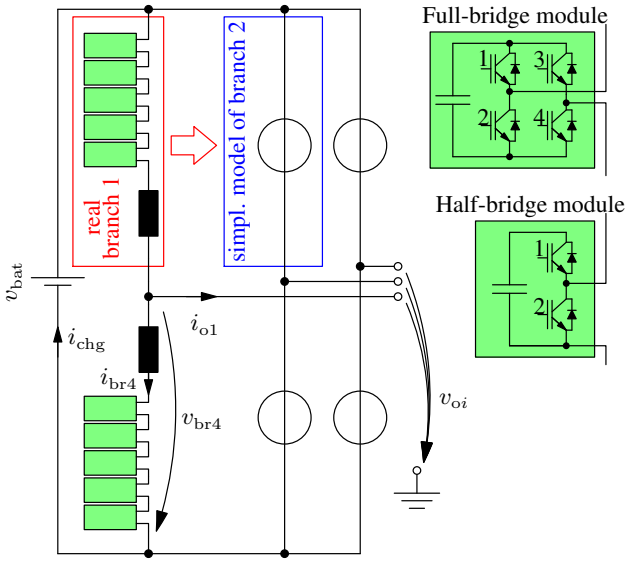


Figure 2: M²LC topology, its simplified model and both types of modules considered

the same voltage and the same switching frequency of $f_s = 750\,\mathrm{Hz}$. With a sufficiently high number of modules per branch, the modules together with a series inductor can be described as continously adjustable voltage sources[4].
With this simplification, it is easily possible to determine currents and voltages in the converter branches. From this knowledge, the installed switching power, the energy variation per branch and the efficiency can be calculated.

## INSTALLED SWITCHING POWER

### CHB without DCDC converter

Here, the sum of maximum module voltages per branch $v_{\mathrm{br,max}}$ depends on the inverter's total nominal battery voltage $v_{\mathrm{bat,N}}$ scaled to its 100% SOC value by $\frac{v_{\mathrm{cell,max}}}{v_{\mathrm{cell,N}}}$:

$$v_{\mathrm{br,max}}^{\mathrm{CHB}} = \frac{v_{\mathrm{cell,max}}}{v_{\mathrm{cell,N}}} \cdot \frac{v_{\mathrm{bat,N}}}{3} \quad . \tag{3}$$

Thus, the sum of the switching power of all IGBTs $P_{\mathrm{sw}}$ is

$$P_{\mathrm{sw}}^{\mathrm{CHB}} = 3 \cdot 4 \cdot v_{\mathrm{br,max}}^{\mathrm{CHB}} \cdot \hat{i}_{\mathrm{o,max}} \tag{4}$$

and has a minimum of 159 MVA at the smallest possible battery voltage. So, the optimal $v_{\mathrm{bat,N}}$ considering $P_{\mathrm{sw}}$ is

$$v_{\mathrm{bat,N,optsw}}^{\mathrm{CHB}} = \frac{v_{\mathrm{cell,N}}}{v_{\mathrm{cell,min}}} \hat{v}_{\mathrm{o}} \quad . \tag{5}$$

### CHB with DCDC converter

Adding a DCDC step-up converter changes the variation in module voltage to $a_{\Delta\mathrm{vcap}}$. Also, the battery voltage needs to be smaller than the module voltage at all times (factor $a_{\mathrm{bsm}} = 0.98$) for proper current decoupling. This gives two lower limits for the peak branch voltage $v_{\mathrm{br,max}}$:

$$v_{\mathrm{br,max}}^{\mathrm{CHB,DCDC}} \geq a_{\Delta\mathrm{vcap}} \hat{v}_{\mathrm{o,max}} \quad \text{and} \tag{6}$$

$$v_{\mathrm{br,max}}^{\mathrm{CHB,DCDC}} \geq \frac{v_{\mathrm{bat,N}}}{3a_{\mathrm{bsm}}} \frac{v_{\mathrm{cell,max}}}{v_{\mathrm{cell,N}}} a_{\Delta\mathrm{vcap}} \quad . \tag{7}$$

Assuming the same switches are used for DCDC converter and output stage, their maximum current $i_{\mathrm{sw,max}}$ has lower limits from both:

$$i_{\mathrm{sw,max}}^{\mathrm{CHB,DCDC}} \geq \frac{P_{\mathrm{inv}}}{v_{\mathrm{bat,N}}} \frac{v_{\mathrm{cell,N}}}{v_{\mathrm{cell,min}}} \quad \text{(DCDC)} \quad \text{and} \tag{8}$$

$$i_{\mathrm{sw,max}}^{\mathrm{CHB,DCDC}} \geq \hat{i}_{\mathrm{o,max}} \quad \text{(output)}. \tag{9}$$

The resulting switching power is a function of $v_{\mathrm{bat,N}}$ and has a (constant) minimum between

$$\underbrace{\frac{P_{\mathrm{inv}}}{\hat{i}_{\mathrm{o,max}}} \frac{v_{\mathrm{cell,N}}}{v_{\mathrm{cell,min}}}}_{23.8\,\mathrm{kV}} \leq v_{\mathrm{bat,N,optsw}}^{\mathrm{CHB,DCDC}} \leq \underbrace{3 \frac{v_{\mathrm{cell,N}}}{v_{\mathrm{cell,max}}} a_{\mathrm{bsm}} \hat{v}_{\mathrm{o,max}}}_{47.4\,\mathrm{kV}} .$$

Below 23.8 kV, the installed switching power is determined by (6) and (8), above 47.4 kV by (7) and (9). The minimum is given by (6) and (9) evaluates to

$$P_{\mathrm{sw,min}}^{\mathrm{CHB,DCDC}} = 18 \cdot a_{\Delta\mathrm{vcap}} \cdot \hat{v}_{\mathrm{o,max}} \cdot \hat{i}_{\mathrm{o,max}} \approx 205\,\mathrm{MVA}.$$

### M$^2$LC with half bridge modules

Using half-bridge modules, the battery voltage must be:

$$v_{\mathrm{bat,N}}^{\mathrm{M^2LCHB}} \geq 2 \frac{v_{\mathrm{cell,N}}}{v_{\mathrm{cell,min}}} \hat{v}_{\mathrm{o,max}} \quad . \tag{10}$$

Battery voltage and output voltage determine the maximum branch voltage:

$$v_{\mathrm{br,max}}^{\mathrm{M^2LCHB}} = \left( \frac{v_{\mathrm{cell,max}}}{2 \cdot v_{\mathrm{cell,N}}} v_{\mathrm{bat,N}}^{\mathrm{M^2LC}} + \hat{v}_{\mathrm{o,max}} \right) \cdot a_{\Delta\mathrm{vcap}} \tag{11}$$

The maximum branch current is equal for upper and lower branch. Assuming a constant charging current, it results in

$$i_{\mathrm{sw,max}}^{\mathrm{M^2LCHB}} = \frac{P_{\mathrm{inv}}}{3 \cdot v_{\mathrm{bat,N}}^{\mathrm{M^2LC}}} \frac{v_{\mathrm{cell,N}}}{v_{\mathrm{cell,min}}} + \frac{\hat{i}_{\mathrm{o,max}}}{2} \tag{12}$$

The installed switching power has a minimum at the minimum possible battery voltage. It is

$$P_{\mathrm{sw}}^{\mathrm{M^2LCHB}} = 6 \cdot 2 \cdot i_{\mathrm{sw,max}}^{\mathrm{M^2LC}} \cdot v_{\mathrm{br,max}}^{\mathrm{M^2LC}} \approx 222\,\mathrm{MVA}.$$

### M$^2$LC with full bridge modules

With full-bridge modules, the limit (10) doesn't apply any more because with negative branch voltages, the output voltage may be greater than half the DC-link voltage. (11) and (12) are still valid. The required switching power

$$P_{\mathrm{sw}}^{\mathrm{M^2LC}} = 6 \cdot 4 \cdot i_{\mathrm{sw,max}}^{\mathrm{M^2LC}} \cdot v_{\mathrm{br,max}}^{\mathrm{M^2LC}} \tag{13}$$

has a minimum at

$$v_{\mathrm{bat,N,optsw}}^{\mathrm{M^2LCFB}} = \frac{2\sqrt{a_{\mathrm{uv}} a_{\mathrm{ov}} a_{\mathrm{vctrl}}} v_{\mathrm{LL,N}} v_{\mathrm{cell,N}}}{\sqrt{3 v_{\mathrm{cell,max}} v_{\mathrm{cell,min}}}} \tag{14}$$

The minimum value is

$$P_{\mathrm{sw,min}}^{\mathrm{M^2LCFB}} = 4 a_{\Delta\mathrm{vcap}} P_{\mathrm{inv}} \left( \frac{v_{\mathrm{cell,max}}}{v_{\mathrm{cell,min}}} + \frac{2 a_{\mathrm{ov}} a_{\mathrm{vctrl}}}{a_{\mathrm{uv}}} + \frac{2\sqrt{2 v_{\mathrm{cell,max}} a_{\mathrm{ov}} a_{\mathrm{vctrl}}}}{\sqrt{v_{\mathrm{cell,min}} a_{\mathrm{uv}}}} \right) \approx 396\,\mathrm{MVA}.$$

## MODULE CAPACITORS

The size of a branch's energy storage is determined by the energy fluctuation, i.e. the difference between the branch energy's maximum and minimum $\Delta e_{\mathrm{br}}$. In this section, the energy fluctuations $\Delta e_{\mathrm{inv}} = \sum \Delta e_{\mathrm{br}}$ occuring in the inverters' DC-links will be evaluated.
However, no attention is paid to smoothing the battery current as this topic is largly depending on battery properties such as surface capacitance, resistance and micro-cycle capability. It should be kept in mind, though, that CHB modules with or without DCDC converter normally should be equipped with a DC-link capacitor to supply high-frequency switching currents. In modules without DCDC converter, the capacitor may even be used to supply the double load frequency current.

## CHB with DCDC converter

With the power transferred through a branch's DCDC converters being constant, the energy variation occuring in the inverter's module capacitors is

$$\Delta e_{\mathrm{inv}} = \frac{S_{\mathrm{inv}}}{\omega_{\mathrm{o}}} \approx 31.8\ \mathrm{kJ} \quad . \tag{15}$$

It is neither a function of the battery voltage nor of the power factor angle $\varphi$.

## M$^2$LC

The dimensioning of the module capacitors for modulation indizes $m \leq 1$ has already been covered by [4]. However, with full-bridge modules, the modulation index is not limited to be $m \leq 1$ (or, with space vector modulation, to $m \leq \frac{2}{\sqrt{3}}$) any more.The derivation is omitted here; however, the results presented below are identical to those presented in [4] for $m \leq 1$. They apply to both full- and half-bridge versions. For compactness, the abbreviations $\mathrm{s}_x = \sin(x)$, $\mathrm{c}_x = \cos(x)$ and $m = \frac{2\hat{v}_{\mathrm{o}}}{v_{\mathrm{bat}}}$ are used.
The energy variation depends on the point of operation: For $m \leq 1$ and $0 \leq \varphi \leq \frac{\pi}{2}$ as well as $1 < m \leq \sqrt{2}$ and $0 \leq \varphi \leq \operatorname{atan}\left(\frac{2-m^2}{2\sqrt{m^2-1}}\right)$,

$$\Delta e_{\mathrm{inv}} = \frac{S_{\mathrm{inv}}}{\omega_{\mathrm{o}}} \frac{\left(4 - m^2\mathrm{c}_\varphi^2\right)^{\frac{3}{2}}}{2m} \quad . \tag{16}$$

For $1 < m \leq \sqrt{2}$ and $\operatorname{atan}\left(\frac{2-m^2}{2\sqrt{m^2-1}}\right) \leq \varphi \leq \frac{\pi}{2}$ as well as $\sqrt{2} \leq m$ and $\operatorname{atan}\left(\frac{m^2-2}{2\sqrt{m^2-1}}\right) \leq \varphi \leq \frac{\pi}{2}$,

$$\Delta e_{\mathrm{inv}} = \frac{S_{\mathrm{inv}}}{4m^2\omega_{\mathrm{o}}} \Big[ m(4 - m^2\mathrm{c}_\varphi^2)^{\frac{3}{2}} + 4\mathrm{c}_\varphi(m^2-1)^{\frac{3}{2}} + (4 + 4m^2 + m^4\mathrm{c}_\varphi^2)\mathrm{s}_\varphi \Big] \tag{17}$$

For $\sqrt{2} \leq m$ and $0 \leq \varphi \leq \operatorname{atan}\left(\frac{m^2-2}{2\sqrt{m^2-1}}\right)$,

$$\Delta e_{\mathrm{inv}} = 2\frac{S_{\mathrm{inv}}}{\omega_{\mathrm{o}}} \frac{\mathrm{c}_\varphi \left(m^2-1\right)^{\frac{3}{2}}}{m^2} \quad . \tag{18}$$

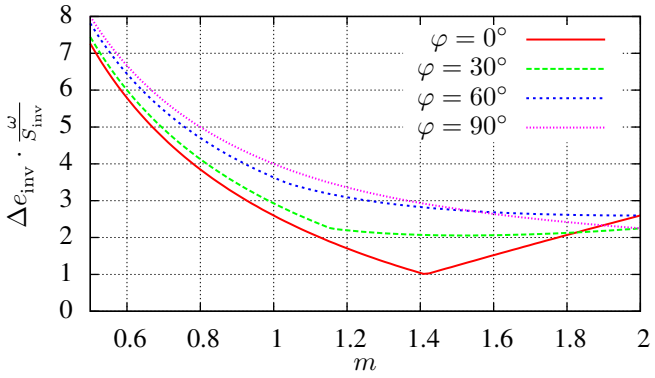


Figure 3: M$^2$LC's energy variation over modulation index for different load angles

These results (fig. 3) have been verified by simulations of the simplified model.

## EFFICIENCY

3.3 kV IGBTs have been chosen as switches for the inverter. They represent a compromise between higher switching power of 6.5 kV devices and good availability and low cost of low voltage switches. As the maximum currents differ between the inverters, assuming the same type of IGBT for all inverters would not be realistic. That is why the FZ1000R33HE, a 1000 A low-loss IGBT made by Infineon[2], has been chosen as reference and scaled to meet the inverters' current requirements. The forward voltages $v_{\mathrm{f}}$ of IGBT and diode are approximated as functions of current using splines.
The number of modules per branch $n_{\mathrm{mpb}}$ results from the switch's reference voltage $v_{\mathrm{ref}}$, see fig. 4:

$$n_{\mathrm{mpb}} = \left\lceil \frac{v_{\mathrm{br,max}}}{v_{\mathrm{ref}}} \right\rceil \tag{19}$$

The average on-times of the single switches are calculated per branch as functions of time $a(t)$.The conduction losses are then evaluated numerically for diode and IGBT of the single switches using

$$P_{\mathrm{c}} = \frac{\omega_{\mathrm{o}}}{2\pi} \int_0^{\frac{2\pi}{\omega_{\mathrm{o}}}} a(t) i(t) v_{\mathrm{f}} \left( i(t) \frac{i_{\mathrm{ref}}}{i_{\mathrm{sw,max}}} \right) \mathrm{d}t \tag{20}$$

with $i(t)$ being the current going through the respective device. The switching losses (IGBT turn-on, IGBT turn-off, diode reverse-recovery) are approximated similarly to the forward voltages according to the datasheet and then evaluated as

$$P_{\mathrm{sw}} = \frac{\omega_{\mathrm{o}} f_{\mathrm{s}}}{2\pi} \frac{v_{\mathrm{br,max}} i_{\mathrm{sw,max}}}{n_{\mathrm{mpb}} v_{\mathrm{ref}} i_{\mathrm{ref}}} \int_0^{\frac{2\pi}{\omega_{\mathrm{o}}}} e_{\mathrm{sw}} \left( i(t) \frac{i_{\mathrm{ref}}}{i_{\mathrm{sw,max}}} \right) \mathrm{d}t.$$

## COMPARISON

Fig. 4 shows superior performance for the standard CHB inverter at first sight. It has the highest efficiency with real power and needs the smallest amount of installed switching power. However, it either exposes the batteries to low-frequency micro-cycles that may reduce their lifetime or it needs huge additional capacitances. Also, it needs the greatest battery voltage (and thus, the largest number of battery cells) for proper operation. This means higher battery managament cost.
Investing about a third of switching power and one inductor per module more by choosing a CHB with DCDC stage leaves only the DCDC converters' high-frequency ripples to the batteries. It allows to considerably reduce the number of battery cells; the number of required modules decreases by 6.Considering the batteries' efficiency, the inverter's increase of losses by half a percent may be acceptable.

The M$^2$LC shows disadvantages in terms of component cost and efficiency. It also doesn't allow to disable a (damaged or empty) part of the battery the way the CHBs do. However, it is worth considering if the inverter is intended not only for connecting the battery but also some other kind of generator to the grid.

In terms of maximum efficiency at an assumed nominal cell voltage of $v_{\mathrm{cell,N}} = \frac{v_{\mathrm{cell,max}}+v_{\mathrm{cell,min}}}{2}$, the CHB with

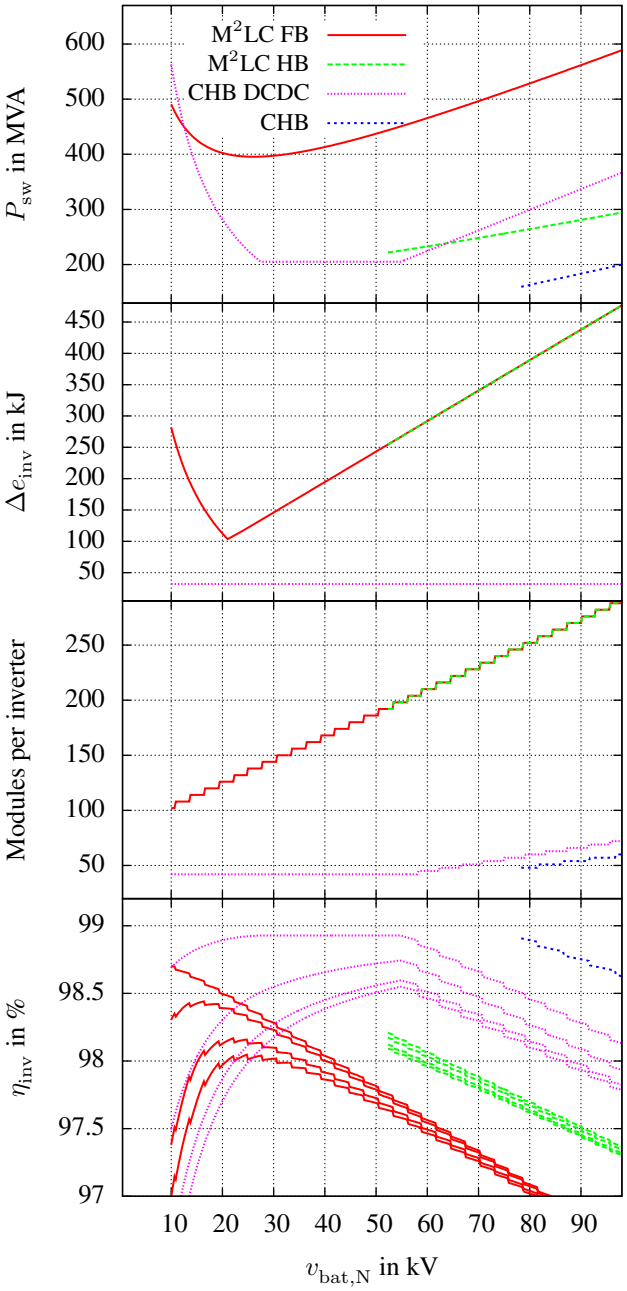


Figure 4: Simulation results: Required switching power (top), worst-case energy variation (below), module count and efficiency (bottom) over the inverter's total nominal battery voltage. In the last plot, the load angle varies between 0° (low eff.) and 90° (high eff.).

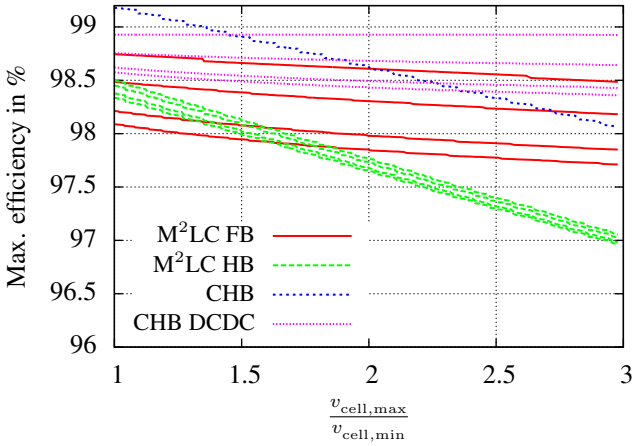


Figure 5: Simulation results: Maximum efficiency at nominal battery voltage over battery voltage variation. Load angle varies between 0° (low eff.) and 90° (high eff.).

DCDC converters and the M$^2$LC with full-bridge modules show advantages for batteries with largly varying voltage (fig. 5). Generally, as long as the battery voltage is fixed, standard topologies are preferable.

## REFERENCES

[1] DIN EN 50160. Leitungsgefuehrte stoergroessen. Deutsches Institut fuer Normung, 2008.

[2] Infineon Technologies AG. *Datasheet FZ1000R33HE3 IGBT*, 2008.

[3] Chih-Chiang Hua, Chun-Wei Wu, and Chih-Wei Chuang. "fully digital control of 27-level cascade inverter with variable dc voltage sources". In *Proc. 2nd IEEE Conf. Industrial Electronics and Applications ICIEA 2007*, pages 2441–2448, 2007.

[4] R. Marquardt, A. Lesnicar, and J. Hildinger. "modulares stromrichterkonzept fuer netzkupplungsanwendungen bei hohen spannungen". In *ETG-Fachtagung, Bad Nauheim*, 2002.

[5] P. Panagis, F. Stergiopoulos, P. Marabeas, and S. Manias. "comparison of state of the art multilevel inverters". In *Power Electronics Specialists Conference, 2008. PESC 2008. IEEE*, pages 4296 –4301, 2008.

[6] N. E. Rueger, H. Kuhn, and A. Mertens. "harmonic distortion of multicarrier pwm strategies in cascaded multilevel converters with unequal dc sources". In *Proc. European Conf. Power Electronics and Applications*, pages 1–10, 2007.

[7] D. U. Sauer. "charging strategies and maintenance for stationary lead-acid batteries". In *Tagungsband Conference Kozienice / Warschau*, 24.03.2006.

[8] L. M. Tolbert, F. Z. Peng, and T. G. Habetler. "multilevel inverters for electric vehicle applications". In *Proc. Power Electronics in Transportation*, pages 79–84, 1998.